



HAL
open science

The problem of the critical angle for edge and center V-notched structures

Alberto Carpinteri, Pietro Cornetti, Nicola Pugno, Alberto Sapora

► **To cite this version:**

Alberto Carpinteri, Pietro Cornetti, Nicola Pugno, Alberto Sapora. The problem of the critical angle for edge and center V-notched structures. *European Journal of Mechanics - A/Solids*, 2011, 10.1016/j.euromechsol.2010.12.017 . hal-00734541

HAL Id: hal-00734541

<https://hal.science/hal-00734541>

Submitted on 23 Sep 2012

HAL is a multi-disciplinary open access archive for the deposit and dissemination of scientific research documents, whether they are published or not. The documents may come from teaching and research institutions in France or abroad, or from public or private research centers.

L'archive ouverte pluridisciplinaire **HAL**, est destinée au dépôt et à la diffusion de documents scientifiques de niveau recherche, publiés ou non, émanant des établissements d'enseignement et de recherche français ou étrangers, des laboratoires publics ou privés.

Accepted Manuscript

Title: The problem of the critical angle for edge and center V-notched structures

Authors: Alberto Carpinteri, Pietro Cornetti, Nicola Pugno, Alberto Sapora

PII: S0997-7538(10)00155-5

DOI: [10.1016/j.euomechsol.2010.12.017](https://doi.org/10.1016/j.euomechsol.2010.12.017)

Reference: EJMSOL 2672

To appear in: *European Journal of Mechanics / A Solids*

Received Date: 16 March 2010

Revised Date: 28 September 2010

Accepted Date: 22 December 2010

Please cite this article as: Carpinteri, A., Cornetti, P., Pugno, N., Sapora, A. The problem of the critical angle for edge and center V-notched structures, *European Journal of Mechanics / A Solids* (2010), doi: [10.1016/j.euomechsol.2010.12.017](https://doi.org/10.1016/j.euomechsol.2010.12.017)

This is a PDF file of an unedited manuscript that has been accepted for publication. As a service to our customers we are providing this early version of the manuscript. The manuscript will undergo copyediting, typesetting, and review of the resulting proof before it is published in its final form. Please note that during the production process errors may be discovered which could affect the content, and all legal disclaimers that apply to the journal pertain.



The problem of the critical angle for edge and center V-notched structures

Alberto Carpinteri, Pietro Cornetti, Nicola Pugno, Alberto Sapora*

Department of Structural Engineering and Geotechnics, Politecnico di Torino,
Corso Duca degli Abruzzi 24, 10129 Torino, Italy

*Corresponding author. Tel.: +39 011 090 4911; fax: +39 011 090 4899

E-mail address: alberto.sapora@polito.it (A. Sapora).

Abstract

In the present paper, the problem of detecting the critical notch angle, i.e. the angle providing the minimum failure load, for brittle or quasi-brittle structures containing either edge or center V-notches is investigated. The expression of the generalized fracture toughness is obtained according to Finite Fracture Mechanics. It is shown that a critical angle is always present: its value depends, through the brittleness number, on both material and geometric characteristics. Thus, the crack is not the most dangerous configuration. The result is supported by experimental results presented in the Literature.

Keywords: Edge and center V-notched structures, Notch sensitivity, Finite Fracture Mechanics

1. Introduction

Many experimental results (Carpinteri, 1987; Seweryn, 1994; Strandberg, 2002; Carpinteri et al., 2008) concerning three-point bending (TPB) and tensile tests on V-notched brittle or quasi-brittle material specimens, show that the failure load does not increase monotonically as the notch opening angle ω increases, but it has a minimum in correspondence of a critical angle ω_c . The problem of determining ω_c was investigated in (Carpinteri et al., 2010) for what concerns an edge V-notched semi-infinite slab and it is here extended to a center V-notched infinite slab under remote tensile load, when the notch is subjected to mode I loading. Four different criteria based on a discrete crack advancement (Seweryn, 1994; Leguillon, 2002; Pugno and Ruoff, 2004; Cornetti et al., 2006) are

taken into account. Despite their predictions slightly differ from each other, all the approaches detect the minimum, whose value depends on the brittleness number s (Carpinteri, 1982): the larger s (i.e. the larger the fracture toughness and/or the smaller the tensile strength and/or the smaller the notch depth), the larger the ω_c expected. A final comparison between theoretical predictions and experimental data confirms the validity of the present analysis.

2. Analysis of semi-infinite edge and center V-notched slabs and different Finite Fracture mechanics criteria

The generalized stress intensity factor (SIF) K_I^* related to an edge V-notched semi-infinite slab or to a center V-notched infinite slab under remote tensile load σ (Fig. 1) can be expressed, by means of dimensional analysis, as (Carpinteri, 1987):

$$K_I^* = \beta(\omega)\sigma a^{1-\lambda(\omega)}, \quad (1)$$

where a is the notch depth in the edge notch case and half of its length in the centre notch case, λ is the solution of the eigen-equation derived by Williams (1952) and β is the shape function, which depends only on the notch angle ω . Values of β related to the two considered geometries can be found tabulated in (Dunn et al., 1997) and they are plotted in Fig. 2 (note that they are modified according to the different definition of the generalized stress-intensity factor here adopted i.e., $\sigma_y(x) = K_I^*/(2\pi x)^{1-\lambda}$ instead of $\sigma_y(x) = K_I^*/x^{1-\lambda}$, xy being the reference system centred at the V-notch tip (Fig. 1)). They differ by a factor 1.12 for $\omega=0^\circ$, while they coincide for $\omega=180^\circ$.

The generalized SIF K_I^* is the coefficient of the dominant term of the stress field at the notch tip and it is expected to be the governing failure parameter within brittle structural behaviour. In other words, failure is supposed to take place whenever (Carpinteri, 1987):

$$K_I^* = K_{Ic}^*, \quad (2)$$

K_{Ic}^* being the generalized fracture toughness. A theoretical justification of this fracture criterion (Eq. (2)) may be given in the framework of Finite Fracture Mechanics (FFM). According to FFM, fracture does not propagate continuously but by finite crack extensions Δ , leading to the following general relationship (Carpinteri et al. 2008; 2010)

$$K_{Ic}^* = \zeta(\omega) \frac{K_{Ic}^{2(1-\lambda)}}{\sigma_u^{1-2\lambda}}, \quad (3)$$

where $\zeta(\omega)$ is a dimensionless function depending on the fracture criterion used, while K_{Ic} and σ_u are the fracture toughness and tensile strength, respectively. It is interesting to notice that also other approaches in the Literature (Sih and Ho, 1991; Lazzarin and Zambardi, 2001) may be grouped into the expression provided by Eq. (3).

Different critical distances Δ and $\zeta(\omega)$ functions, according to different FFM approaches, are summarized in Table 1: they refer to the average stress (LS) criterion (Seweryn, 1994), the average energy (LE) criterion (Pugno and Ruoff, 2004; Taylor et al., 2005), the coupled point stress and average energy (PSLE) criterion (Leguillon, 2002), and the coupled average stress and average energy (LSLE) criterion (Cornetti et al., 2006).

The energy-based criteria all involve a dimensionless coefficient μ , depending on the notch angle ω , which rises from the evaluation of the SIF for a short crack of length e at the V-notch, $K_I = \mu(\omega) K_I^* e^{\lambda-1/2}$ (Hasebe and Iida, 1978). Accurate values of μ can be found tabulated either in (Philipps et al., 2008) or, in the present notation, in (Carpinteri et al., 2010). It increases from unity, when $\omega = 0^\circ$, up to $1.12\sqrt{\pi}$, when $\omega = 180^\circ$. On the other hand, the constant c appearing according to the LE criterion is equal to 1.12.

Observe that the critical distances related to the LS and LE criteria are material properties, while Δ becomes a structural parameter, depending, through λ and μ , also on the notch opening angle ω , for what concerns the coupled criteria.

Inserting Eqs. (1) and (3) into Eq. (2), yields:

$$\frac{\sigma_f}{\sigma_u} = \frac{\zeta}{\beta} \alpha^{\lambda-1}, \quad (4)$$

where σ_f is the remote stress at failure and α is the dimensionless notch depth

$$\alpha = \frac{1}{s^2} = a \left(\frac{\sigma_u}{K_{Ic}} \right)^2. \quad (5)$$

The brittleness number $s = K_{Ic}/(\sigma_u \sqrt{a})$ was introduced by Carpinteri (1981a,b). It shows, in a synthetic way, that brittleness is more a structural property rather than a material one: structural

failure is brittle not only for low toughness and high tensile strength materials (i.e., brittle materials), but also for large specimen sizes. According to its definition, low brittleness numbers generally correspond to brittle structural behaviours. In the present case, i.e. infinite or semi-infinite slabs, the characteristic structural size a coincides with the notch depth, the only relevant size in the problem.

3. Discussion on the critical angle

The critical notch angle could be determined by deriving Eq. (4) with respect to ω and imposing the stationary condition. The following relationship is obtained:

$$\alpha = \frac{1}{s^2} = \exp \left[\frac{1}{\lambda'} \left(\frac{\beta'}{\beta} - \frac{\zeta'}{\zeta} \right) \right] \Bigg|_{\omega = \omega_c} \quad (6)$$

By evaluating the derivatives λ' , β' and ζ' , the inverse of Eq. (6) is plotted in Figs. 3 and 4, for the two geometries considered, providing the value of the critical notch opening angle ω_c for a given α (or s) value. As it can be observed, in both the cases, ω_c depends through s both on the material and the geometry. It is evident that the crack is the most dangerous V-notch ($\omega_c=0^\circ$) only for extremely large notches and/or very brittle materials (i.e., low fracture toughness and/or high tensile strength). All the FFM criteria are able to catch the minimum, although their predictions slightly differ from each other. Particularly, the PSLE approach generally provides the lowest ω_c values, while the highest ω_c values are obtained through the LSLE criterion. Eventually, observe that, for a given α , higher predictions are expected for what concerns the center-notch case.

The problem could also be analyzed from the opposite point of view, that is by varying α (i.e., s), and keeping ω fixed in Eq. (4). For the sake of clarity, only the results obtained by applying the LSLE approach to the semi-infinite edge-notched slab are plotted in Fig. 5. It is evident that the minimum failure load is provided by the edge crack case only for $\alpha \rightarrow \infty$ ($s \rightarrow 0$), whereas it corresponds to the flat edge for $\alpha \rightarrow 0$ ($s \rightarrow \infty$). In the intermediate cases, the minimum failure load is provided by a V-notch of amplitude ω_c ranging from 0° up to 180° as α decreases from infinite to zero. In Fig. 5 also the envelope has been drawn, i.e. the line that is tangent to all the diagrams plotted keeping ω fixed, which provides the minimum achievable relative failure stress for each relative notch depth α . The graphic related to the center-notch case is very similar. Furthermore, the use of different FFM criteria, from a qualitative point of view, does not affect the results.

4. Comparison with experimental data

In this section, a comparison between experiments and theoretical predictions by different FFM criteria is performed. In the case of finite geometries, by means of dimensional analysis, Eq. (4) can be rewritten as:

$$\frac{P_{cr}^{\omega}}{P_{cr}^{\pi}} = \frac{\zeta(\omega)}{f(a/h, l/h, \omega)} s^{2(1-\lambda)} \quad (7)$$

where P_{cr}^{ω} and P_{cr}^{π} are the failure loads for a notch opening angle equal to ω and 180° , respectively, h is the specimen height and l its length. The shape function f replacing β , depends now not only on the amplitude but also on the relative notch depth and the slenderness ratio. Indeed, this latter dependence is practically negligible for TPB specimens with $l/h > 8$ and for tensile specimens with $l/h > 2$ (Tada et al., 1985). The brittleness number now recovers the usual expression $s = K_{Ic}/(\sigma_u \sqrt{h})$. It is important to point out that, if the notch and the ligament depths are sufficiently large with respect to the finite crack extension Δ , the functions $\zeta(\omega)$ obtained for infinite geometries and reported in Table 1 could be also applied to finite geometries (Eq. (7)), without loosing of generality (Seweryn, 1994; Carpinteri et al., 2008).

All the experimental data here considered (Carpinteri, 1987; Seweryn, 1994; Strandberg, 2002; Carpinteri et al., 2008) share the following common features:

- The samples contain a sharp edge V-notch: the notch radius is small enough not to affect the results. Moreover, specimens referring to TPB tests show a slenderness ratio $l/h \sim 4$, while, for tensile tests, $l/h > 2$.
- The loading is applied in mode I and fracture is of a brittle character.
- The presence of a critical angle ω_c rises from the evaluated failure loads, which do not increase strictly monotonically as a function of the notch opening angle ω .

TPB tests on V-notched PMMA specimens carried out by Carpinteri (1987), for instance, show the minimum failure load for $\omega_c \sim 45^{\circ}$ (Fig. 6a). Similar results ($\omega_c \sim 40^{\circ}$) are obtained by Seweryn (1994), testing double-edge notched tension (DENT) PMMA samples (Fig. 6b). Strandberg (2002) performed tests on single edge notched tension (SENT) specimens made of soft annealed tool steel at -50°C . Although, in this case, the cracked specimens are the ones providing the minimum failure

load, this lowest value, according to the Author himself, is due to the pre-cracking procedure carried out to manufacture the cracked specimen and to a crack depth deviating by +16% from that related to the other tested geometries. For this reason, the fracture toughness value (as well as that of the tensile strength) was obtained from a best fit procedure in (Strandberg, 2002). The same will obviously apply in the present study (Table 2). Moreover, since the failure load slightly decreases by passing from 30° to 60° and afterwards it increases monotonically with ω , $\omega_c \sim 60^\circ$ can be regarded as a minimum (Fig. 6c). Eventually, TPB tests carried out on polystyrene specimens (Carpinteri et al., 2008) do not show a significant difference between the failure loads for the 60° -notch sample and the 120° -notch sample (Fig. 6d) and the presence of a minimum between these two cases can be supposed.

The structural properties, for all the experiments here considered, are reported in Table 2. As it can be observed by evaluating the square ratio of the fracture toughness to the tensile strength, PMMA ($(K_{Ic}/\sigma_u)^2 \approx 0.26-0.32 \cdot 10^{-3} \text{m}$) is more brittle than the other two materials ($(K_{Ic}/\sigma_u)^2 \approx 0.90 \cdot 10^{-3} \text{m}$). The dimensions of the TPB and DENT PMMA specimens are quite similar and sensibly larger than those related to the other tests. Moreover, the same occurs for what concerns the dimensionless notch depth a/h , which is equal to 0.40-0.50, 0.16 and 0.10 for PMMA, steel and polystyrene samples, respectively. All these considerations can be synthesized by referring to the values assumed by the brittleness number s (Table 2), which shows that the structural response was really brittle for PMMA specimens, and less brittle for the other material specimens.

In Fig. 6 there are reported the FFM predictions by means of Eq. (7). Shape functions f are obtained either numerically (Sinclair et al., 1984) or by exploiting those already evaluated, as done for steel samples (Strandberg, 2002): in this case, however, the shape function related to the crack-case has been re-calculated (Tada et al., 1985). As it can be seen, a good agreement is generally found between experimental data and theoretical predictions. The highest values for the relative failure loads are provided by the PSLE criterion: its predictions slightly differ from those obtained by the other FFM criteria, which result to be very close. Notice that the LSLE approach always provides the lowest values.

These behaviours also reflect on the critical angle ω_c value. For smaller s , although the difference between the theoretical predictions related to different notched geometries with $0^\circ < \omega < 60^\circ$ is not so significant (Figure 6), all the FFM criteria are able to catch the minimum (Table 2) and similar results are obtained. While for DENT PMMA samples the theoretical critical value ω_c is close to the experimental one, for TPB PMMA specimens is lower. Note anyway, that no specimens with notch amplitude comprised between 0° and 45° were tested in (Carpinteri, 1987).

For higher s (steel and polystyrene), the ω_c predictions according to different FFM approaches slightly differ, especially those provided by the PSLE criterion. Observe from Table 2 that the general trend obtained in Fig. 3 (i.e., the semi-infinite edge-notched geometry) is coherently recovered. Furthermore the minimum is more marked (Figure 6): referring to TPB tests on polystyrene specimens and to the LSLE criterion predictions (which always result to be the closest to the experimental values), for instance, the difference between the failure loads for the 0° -notch sample and for the 87° -notch sample (which provides the minimum, Table 2) is approximately 4%. Eventually, taking into account the same test and the same criterion, Eq. (7) has been plotted in Fig. 7 by varying ω and keeping s fixed. It can be thought that different curves refer to specimens with the same geometry of the polystyrene samples tested in (Carpinteri et al., 2008), for which $s=0.236$, but with different material properties. It is clear that, also for finite geometries, there exists a critical notch angle ω_c , whose position moves from 0° to 180° as the brittleness number s increases. For less brittle structural behaviours, the minimum is more pronounced. On the other hand, for very large s values (i.e. ductile structural behaviours), the FFM predictions provide failure loads higher than that for plain specimens and therefore unacceptable, despite the failure load at the minimum is always lower than P_{cr}^π .

5. Conclusions

The presence of a critical angle providing the minimum failure load, in brittle or quasi-brittle structures containing edge and center re-entrant corners, is investigated. The study concerns both infinite and finite geometries, under different loading conditions. It is shown that a critical angle always exists and is more pronounced for large s values (i.e. relatively ductile materials and/or small structural sizes), while it becomes almost imperceptible for small s values: only in this case the crack tends to become the most dangerous configuration.

Acknowledgments

The financial support of the Italian Ministry of Education, University and Research (MIUR) to the Project “Advanced applications of Fracture Mechanics for the study of integrity and durability of materials and structures” within the “Programmi di ricerca scientifica di rilevante interesse nazionale (PRIN)” program for the year 2008 is gratefully acknowledged.

References

- Carpinteri, A., 1981a. Size effect in fracture toughness testing: a dimensional analysis approach. In: Sih, G.C., Mirabile, M. (Eds.), *Analytical and Experimental Fracture Mechanics (Proceedings of the International Conference on Analytical and Experimental Fracture Mechanics, Roma, Italy, 1980)*. Sijthoff & Noordhoff, Alphen aan den Rijn, pp. 785–797.
- Carpinteri, A., 1981b. Static and energetic fracture parameters for rocks and concretes. *Mater. Struct.* 14, 151-62.
- Carpinteri, A., 1987. Stress-singularity and generalized fracture toughness at the vertex of re-entrant corners. *Eng. Fract. Mech.* 26, 143-155.
- Carpinteri, A., Cornetti, P., Pugno, N., Sapora, A., Taylor, D., 2008. A finite fracture mechanics approach to structures with sharp V-notches. *Eng. Fract. Mech.* 75, 1736-1752.
- Carpinteri, A., Cornetti, P., Pugno, N., Sapora, A., 2010. On the most dangerous V-notch. *Int. J. Solids Struct.* 47, 887-893.
- Cornetti, P., Pugno, N., Carpinteri, A., Taylor, D., 2006. Finite fracture mechanics: a coupled stress and energy failure criterion. *Eng. Fract. Mech.* 73, 2021-2033.
- Dunn, M., Suwito, W., Cunnigham, S., 1997. Stress intensities at notch singularities. *Eng. Fract. Mech.* 57, 417-430.
- Hasebe, N., Iida, J., 1978. A crack originating from a triangular notch on a rim of a semi-infinite plate. *Eng. Fract. Mech.* 10, 773-782.
- Lazzarin P., Zambardi R., 2001. A finite-volume-energy based approach to predict the static and fatigue behavior of components with sharp v-shaped notches. *Int. J. Fract.* 112, 275-298.
- Leguillon, D., 2002. Strength or toughness? A criterion for crack onset at a notch. *Eur. J. Mech. A/Solids.* 21, 61-72.
- Philipps, A.G., Karuppanan, S., Churchman, C.M, Hills, D.D., 2008. Crack tip stress intensity factors for a crack emanating from a sharp notch. *Eng. Fract. Mech.* 75, 5134-5139.
- Pugno, N., Ruoff, R., 2004. Quantized fracture mechanics. *Philos. Mag.* 84, 2829-2845.
- Seweryn, A., 1994. Brittle fracture criterion for structures with sharp notches. *Eng. Fract. Mech.* 47, 673-681.
- Sih G.C., Ho J.W., 1991. Sharp notch fracture strength characterized by critical energy density. *Theor. Appl. Fract. Mec.* 16, 179-214.
- Sinclair, G., Okajima, M., Griffin, J., 1984. Path independent integrals for computing stress intensity factors at sharp notches in elastic plates. *Int. J. Numer. Meth. Engng.* 20, 999-1008.
- Strandberg, M., 2002. Fracture at V-notches with contained plasticity. *Eng. Fract. Mech.* 69, 403-415.

- Tada, H., Paris, P., Irwin, G., 1985. The stress analysis of cracks. Handbook. Paris Productions Incorporated, St Louis.
- Taylor, D., Cornetti, P., Pugno, N., 2005. The fracture mechanics of finite crack extension. Eng. Fract. Mech. 72, 1021-1038.
- Williams, M.L., 1952. Stress singularities resulting from various boundary conditions in angular corners of plate in extension. J. Appl. Mech. 19, 526-528.

Table captions:

Table 1: Different critical distances l and ξ functions and according to different FFM criteria.

Table 2. Structural properties related to the experimental data considered and critical angle values ω_c obtained experimentally and through different FFM criteria.

(*) For DENT specimens h denotes half of the total height

Figure captions:

Fig. 1: Geometry of tensile slabs: a) semi-infinite edge-notched b) infinite center-notched.

Fig. 2: Function β vs. notch opening angle ω (degrees) for a semi-infinite edge notched slab (thin line) and for an infinite center-notched slab (thick line) under remote tensile load.

Fig. 3: Semi-infinite edge-notched slab under remote tensile load: critical notch-opening angle ω_c (degrees) vs. dimensionless notch depth α according to different FFM criteria.

Fig. 4: Infinite center-notched slab under remote tensile load: critical notch-opening angle ω_c (degrees) vs. dimensionless notch depth α according to different FFM criteria.

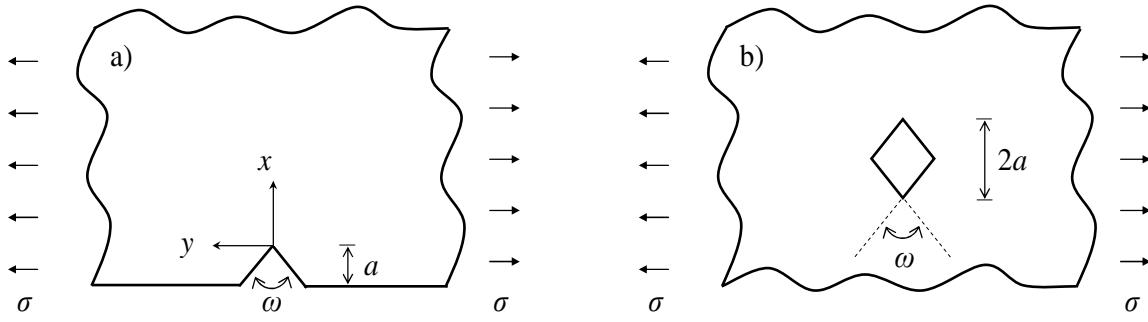
Fig. 5: Relative failure load $P_{cr}^{\omega}/P_{cr}^{\pi}$ vs. dimensionless notch depth $\alpha=1/s^2$ for a semi-infinite edge-notched slab, according to the LSLE criterion. The black thick line represents the envelope of the other curves.

Fig. 6: Relative failure load $P_{cr}^{\omega}/P_{cr}^{\pi}$ vs. notch opening angle ω (degrees) for different experimental tests: a) TPB, PMMA b) DENT, PMMA c) SENT, steel d) TPB, polystyrene. Experimental data (asterisks) and predictions related to different FFM criteria: LS (dashed line), LE (continuous thin line), PSLE (dotted line) and LSLE (continuous thick line). Circles represent the minimum relative failure load according to the LSLE criterion.

Fig. 7: Relative failure load $P_{cr}^{\omega}/P_{cr}^{\pi}$ vs. notch opening angle ω (degrees), according to the LSLE criterion, for increasing values of the brittleness number s . Results refer to specimens possessing the same geometry of the polystyrene samples tested in (Carpinteri et al. 2008), here represented by the $s=0.236$ curve. The thick line represents the locus of the minima.

Criterion	LS	LE	PSLE	LSLE
Failure condition	$\int_0^\Delta \sigma_y(x) dx = \sigma_u \Delta$	$\int_0^\Delta K_I^2(e) de = K_{Ic}^2 \Delta$	$\begin{cases} \sigma_y(x = \Delta) = \sigma_u \\ \int_0^\Delta K_I^2(e) de = K_{Ic}^2 \Delta \end{cases}$	$\begin{cases} \int_0^\Delta \sigma_y(x) dx = \sigma_u \Delta \\ \int_0^\Delta K_I^2(e) de = K_{Ic}^2 \Delta \end{cases}$
Δ	$\frac{2}{\pi} \left(\frac{K_{Ic}}{\sigma_u} \right)^2$	$\frac{2}{\pi c} \left(\frac{K_{Ic}}{\sigma_u} \right)^2$	$\frac{2\lambda}{\mu^2 (2\pi)^{2(1-\lambda)}} \left(\frac{K_{Ic}}{\sigma_u} \right)^2$	$\frac{2}{\lambda \mu^2 (2\pi)^{2(1-\lambda)}} \left(\frac{K_{Ic}}{\sigma_u} \right)^2$
$\zeta(\omega)$	$\lambda 4^{1-\lambda}$	$\frac{c\sqrt{\pi}\lambda}{\mu} \left(\frac{2}{\pi c^2} \right)^{1-\lambda}$	$\lambda^{1-\lambda} \left[\frac{(2\pi)^{2\lambda-1}}{\mu^2/2} \right]^{1-\lambda}$	$\lambda^\lambda \left[\frac{(2\pi)^{2\lambda-1}}{\mu^2/2} \right]^{1-\lambda}$

Tests	TPB, PMMA	DENT, PMMA	SENT, steel	TPB, polystyrene
l (m)	0.1900	0.1920	0.1300	0.0760
h (m)	0.0500	0.0545 ^(*)	0.0300	0.0180
a (m)	0.0200	0.0270	0.0050	0.0018
σ_u (MPa)	123.80	104.90	2006.00	70.61
K_{Ic} (MPa \sqrt{m})	1.92	1.86	58.24	2.23
s	0.0693	0.0759	0.168	0.236
ω_c (exp.)	~45°	~40°	~60°	-
ω_c (LS)	24°	30°	48°	75°
ω_c (LE)	25°	32°	49°	80°
ω_c (PSLE)	21°	24°	32°	45°
ω_c (LSLE)	25°	34°	54°	87°



ACCEPTED MANUSCRIPT

